Tensor effective interaction in self-consistent Random Phase Approximation calculations

M. Anguiano[1], G. Co' [2,3], V. De Donno [2,3] and A. M. Lallena[1]

1) Departamento de Física Atómica, Molecular y Nuclear,

Universidad de Granada, E-18071 Granada, SPAIN

2) Dipartimento di Fisica, Università del Salento, Via Arnesano, I-73100 Lecce, ITALY

3) INFN, Sezione di Lecce, Via Arnesano, I-73100 Lecce, ITALY

(Dated: February 15, 2011)

Abstract

We present a study of the effects of the tensor-isospin term of the effective interaction in Hartree-Fock and Random Phase Approximation calculations. We used finite-range forces of Gogny type, and we added to them a tensor-isospin term which behaves, at large internucleonic distances, as the analogous term of the microscopic interactions. The strength of this tensor force has been chosen to reproduce the experimental energy of the lowest 0^- excited state in ^{16}O, which shows large sensitivity to this term of the interaction. With these finite-range interactions, we have studied the effects of the tensor-isospin force in ground and excited states of carbon, oxygen, calcium, nickel, zirconium, tin and lead isotopes. Our results show that the tensor force affects mainly the nucleon single particle energies. However, we found some interesting cases where also bulk nuclear properties are sensitive to the tensor interaction.

PACS numbers:

I. INTRODUCTION

At the beginning of the 40's of the past century, the existence of the electric quadrupole moment of the deuteron [1, 2] was explained by Rarita and Schwinger by introducing a static tensor term in the nucleon-nucleon (N-N) interaction [3, 4]. Since then, tensor terms are unavoidable ingredients of the microscopic N-N interactions, i.e. those interactions constructed to reproduce the properties of two-nucleon systems.

Despite their relevance in microscopic interactions, the tensor terms are usually neglected when effective interactions and theories are used. In the effective theories some complicated many-body effects are treated, obviously in effective and average manner, by changing the values of the parameters of the interaction. Some specific observables of the nucleus are chosen to select these values. For example, in Hartree-Fock calculations these observables are usually the nuclear binding energies. The effective theory is expected to be able to describe other observables. If this fails, one searches for many-body effects which should be explicitly treated to improve the description of the data. In this manner, we link many-body effects to specific observables. In the case of our interest here, the tensor force, the point is the identification of observables clearly depending on the presence of this term in the effective N-N interaction.

In these last years, the interest on the tensor terms of the effective N-N interaction has increased because the inclusion of these terms improves the description of the single particle (s.p.) energies of some isotope or isotone chains [5–8] when the Hartree-Fock theory is used [9–15].

We see some weak points in using the s.p. energies to define the strength of the tensor terms of the effective interactions. First, s.p. energies are extremely sensitive to the spin-orbit terms of the N-N interaction, and this obscures the possibility of a clear identification of the tensor effects (see for example the discussion in Ref. [16]). Furthermore, observations are always done on global nuclear properties, therefore the identification of the measured quantities with s.p. properties of the nucleus is done by imposing to the observed quantity the physical interpretation given within a mean field description of the many-body system. The fact that experimental values of spectroscopic factors are usually rather different from the mean field expectations is a clear indication of the limits of this procedure.

In this article we propose an alternative approach to select the strength of the effective

tensor forces. We have looked at the excitation spectrum to find observables particularly sensitive to the tensor force. We have identified these observables with the energies of the 0^- charge conserving excitations. By using a recursive self-consistent Hartree-Fock (HF) plus Random Phase Approximation (RPA) procedure, we have chosen the strength of the tensor term of the effective interaction to reproduce the experimental value of the 0^- in ^{16}O. With these new interactions we have investigated the ground and excited state properties of various nuclei by doing HF plus RPA calculations.

The structure of the tensor terms we have considered and the methodology used to select their strengths are presented in Sec. II. We discuss the results obtained in the description of the ground states of various nuclei in Sec. III, and in Sec. IV the results obtained for the excited states. We summarize the main points of our work and draw our conclusions in Sec. V.

II. THE INTERACTION

The most important tensor component of the microscopic N-N interaction is that related to the tensor-isospin channel [17, 18] whose long range behaviour is dominated by the exchange of a single pion. Since the pion is the lightest meson, the range of the tensor-isospin term is longer than the ranges of the other terms of the N-N interaction. For this reason we have chosen to consider, in our effective interactions, only tensor-isospin terms with finite range. The use of finite range forces requires, in both HF and RPA calculations, the evaluation of direct and exchange interaction matrix elements.

The tensor-isospin term of our effective interaction is based on the analogous term of the microscopic Argonne V18 interaction [18]. We have multiplied the radial part of this term by a function which simulates the effect of the short-range correlations [19]. In our work, the radial part of the tensor-isospin term has the form

$$v_6(r) \,=\, v_{6,\mathrm{AV18}}(r)\,\left[1 \,-\, \exp\left(-\,b\,r^2\right)\right]\,, \tag{1}$$

where we have indicated with r the distance between the two interacting nucleons, with $v_{6,\mathrm{AV18}}$ the radial function of the Argonne V18 tensor-isospin potential [18], and with b a free parameter. The changes in the tensor-isospin term produced by choosing different values of b are shown in panel (a) of Fig. 1, where we present the Fourier transformed function

$V_6(q)$, defined by the equation

$$V_6(q)\, S_{12}(\mathbf{q}) \;=\; \int \mathrm{d}^3 r\, \exp\left(i\,\mathbf{q}\cdot\mathbf{r}\right)\, v_6(r)\, S_{12}(\mathbf{r}) \\ =\; -\,4\pi \int \mathrm{d}r\, r^2\, j_2(qr)\, v_6(r)\, S_{12}(\mathbf{r})\,. \qquad (2)$$

In the above equation r and q indicate the moduli of $\mathbf{r}$ and $\mathbf{q}$, and we used the definition of the tensor operator

$$S_{12}(\mathbf{r}) \;=\; 3\,\frac{[\boldsymbol{\sigma}(1)\cdot\mathbf{r}]\,[\boldsymbol{\sigma}(2)\cdot\mathbf{r}]}{r^2} \;-\; \boldsymbol{\sigma}(1)\cdot\boldsymbol{\sigma}(2)\,, \qquad (3)$$

where $\boldsymbol{\sigma}$ are the usual Pauli spin matrices.

The results presented in the panel (a) of Fig. 1 show that the correlation effects reduce the strength of the bare tensor force. The smaller is the value of b, the more extended in r space is this effect, therefore the function to be integrated in Eq. (2) becomes smaller.

The first step of our study consisted in identifying an observable very sensitive to the tensor force with the aim of using it to determine the strength of this part of the effective interaction. We have conducted this study by investigating the excitation spectra of the ^{12}C, ^{16}O, ^{40}Ca, ^{48}Ca, ^{90}Zr and ^{208}Pb nuclei within the phenomenological RPA approach developed by the Jülich group [20, 21]. In this approach, based on the Landau-Migdal theory of finite Fermi systems [22], the set of s.p. energies and states is obtained by using phenomenological mean field potentials that, in our case, have the shape of Woods-Saxon wells. The values of the parameters of the potential are chosen for each nucleus in order to reproduce at best the empirical values of the s.p. energies around the Fermi surface and the values of the charge root mean square radii. The explicit expression of the potential, and the values of the parameters, can be found in Refs. [19, 23]. Following the philosophy of the Landau-Migdal approach, in the RPA calculations we substituted the Woods-Saxon s.p. energies with their experimental values, when they are available.

All the RPA results presented in this article have been obtained by using a discrete s.p. basis. In the phenomenological calculations discussed in this section we have used a discrete s.p. basis obtained by diagonalizing the Woods-Saxon well in a harmonic oscillator basis. In analogy with the work of Ref. [23], we have used configuration spaces large enough that the inclusion of additional s.p. states does not modify the energies of the first excited states, below 20 MeV in the lighter nuclei and 15 MeV in the heavier ones, within 0.1 MeV.

In these phenomenological calculations we used as basic N-N effective interaction a density dependent Landau-Migdal force. The values of the force parameters, given in Refs. [23, 24], change for each nucleus, and are chosen to reproduce at best the energies of the collective low-lying 3^- states of each nuclei, and also the energies of the 12^- excited states in ^{208}Pb. We added to this basic interaction a tensor term of the form given by Eq. (1), and we studied the excitation spectra of the nuclei mentioned above.

In agreement with previous calculations [21, 25] we observed that the influence of the tensor term on the natural parity states is negligible. We found few cases of interest in the spectrum of the unnatural parity excitations. The most interesting one was the excitation of the 0^- states, which show common characteristics in all the nuclei we considered.

In Fig. 2 we have summarized the results obtained for the energies of the lowest 0^- excitations in the nuclei investigated. In this figure, the squares indicate the values of the 0^- excitation energies, obtained by adding the tensor term of Eq. (1) to the Landau-Migdal force, as a function of the parameter b. The horizontal dashed lines indicate the values obtained without tensor term, while the dotted lines show the values obtained by using the full tensor term of the Argonne V18 interaction. The full lines show the experimental values [26, 27].

We observe that the effect of the tensor term is always attractive, i.e. all the energies obtained with the tensor terms are smaller than those obtained without it. The values of these energies decrease, monotonically and smoothly, from the dashed to the dotted lines when the value of b increases, as we have naively expected. Discussing the results in more detail, we have obtained variations of the energies from 4 up to 8 MeV, and, in relative variations, between 30% and 100%. These are the largest effects of the tensor force on the excitation energies we have found in our investigation. In the ^{48}Ca case, the effect of the full tensor term is so strong that we obtained an imaginary solution for the RPA equations.

The remarkable sensitivity of the 0^- excitation energies to the presence of the tensor force, and their smooth behaviour with respect to the changes of its strength, make these energy values particularly suitable to be chosen as experimental benchmarks to select the strength of the tensor terms in effective interactions.

In this work we have performed HF plus RPA calculations. The HF equations were solved with the method used in Refs. [28, 29]. This method is based on the plane wave expansion technique developed by Guardiola and Ross [30, 31]. After the iterative process

has reached the convergence, we solved the HF differential equations not only for the s.p. states below the Fermi level, the hole states, but also for those states above the Fermi level, the particle states. The numerical method automatically produces a set of discrete levels even when the s.p. energies are larger than zero, i.e. in the continuum region. We did not find general criteria for the stability of our results. This problem is not very important in the phenomenological RPA approach, since the effects related to the truncation of the s.p. configuration space are taken into account by changing the parameters of the force. However, in self-consistent calculations this is a more serious problem, since the interaction parameters are chosen to reproduce, in HF calculations, the ground state properties of the various nuclei, and the force remains unchanged in RPA calculations.

To keep under control these problems, we restricted our study to the low-lying excited states. For each excitation studied we used the same criterion considered in the phenomenological approach, i.e. we controlled that the energy eigenvalues of the first low-lying states did not vary by more than 0.1 MeV against the enlargement of the configuration space. In order to obtain this numerical accuracy, we had to use configuration spaces composed by a few thousands s.p. states, more than 2000 in ^{208}Pb. The numerical stability of higher energy excitations, such as giant resonances, requires even larger configuration spaces. In this case we believe it is necessary to abandon the discrete RPA calculations and treat correctly the continuum, as it is done, for example, in Refs. [32, 33].

We have built two new forces by adding to the D1S [34] and D1M [35] parameterizations of the Gogny interaction [36] a tensor-isospin term similar to that given by Eq. (1). We label D1ST and D1MT these new interactions. Since in Gogny-like forces the spin-orbit term is fixed to reproduce the experimental splitting of the s.p. energies of the $1p_{1/2}$ and $1p_{3/2}$ neutron states in ^{16}O, we used this nucleus as reference. The new interactions have been fixed by using an iterative procedure. We started with a HF calculation without tensor force to produce a set of s.p. energies and wavefunctions to be used in the RPA calculations. Then, we made a RPA calculation with the tensor force and we fixed the value of the parameter b of Eq. (1) in order to reproduce the energy of the first 0^- excitation of ^{16}O at 10.6 MeV. With this new interaction we recalculated the HF s.p. energies by changing the spin-orbit interaction to reproduce the splitting of the two p states quoted above. These HF and RPA calculations have been repeated until the convergence of the result was obtained. By using this procedure we have found for the parameter b the value 0.6 fm^{-2}, for the D1ST

force, and of 0.25 fm^{-2}, for the D1MT one. Summarizing, we added a tensor term to the D1S and D1M Gogny-like interactions and we modified only the spin-orbit terms from 130 MeV, in the original D1S force, to 134 MeV, in the D1ST interaction, and from 115 MeV, in the D1M force, to 122.5 MeV, in the D1MT interaction. No other values of the force parameters have been changed.

The tensor terms of the D1ST and D1MT interactions are indicated in panel (b) of Fig. 1 by the dashed-dotted and dashed-doubly-dotted lines respectively. In this figure they are compared with the tensor-isospin term of the microscopic Argonne V18 interaction (solid curve). By construction, the effective tensor terms are smaller than that of the bare N-N interaction. More interesting is the comparison with the long dashed line which has been produced by multiplying the bare interaction with the scalar part of the short-range correlation function obtained in Correlated Basis Function calculations [19]. The remarkable difference between this line and those of the D1ST and D1MT forces indicates that our procedure includes in the effective tensor term not only the effects of the short-range correlations, but also some other many-body effects that the microscopic calculations consider explicitly. In the same panel we make a comparison with other two tensor terms of finite-range interactions used in the literature, the GT2 [10] and the M3YP2 [37] forces. The tensor term of the GT2 is constructed to have the same volume integral of the Argonne V18 tensor force. The strength of this tensor force is much larger than those of the tensor forces we have built. On the opposite, we observe that the tensor term of the M3YP2 force is much smaller.

Even though the D1ST and D1MT forces reproduce the experimental value of the excitation energy of the 0^- state at 10.6 MeV in ^{16}O, they produce rather different RPA wave functions, as we have verified by calculating transition densities and inclusive neutrinos cross sections for this excited state.

III. HARTREE-FOCK RESULTS

We used the D1ST and D1MT interactions, whose construction has been described in the previous section, to make spherical HF calculations for a set of nuclei in different regions of the isotope chart. We have chosen nuclei where the s.p. states below the Fermi level are fully occupied to avoid deformation problems and to minimize pairing effects. We have verified

these features by controlling the results given by the deformed Hartree-Fock-Bogolioubov calculations of Ref. [38].

In Fig. 3 we compare the binding energies obtained for various nuclei we have considered, with the experimental values taken from Refs. [39, 40]. The experimental energies of the ^{28}O, ^{48}Ni, ^{60}Ca, ^{78}Ni and ^{100}Sn nuclei have not been measured but estimated [40].

The methodology used in our study is already evident. We have investigated the effects of the tensor force by comparing the results obtained by using forces with and without tensor term. To emphasize the effects of the tensor force, we show in the panel (a) of Fig. 3 the quantity

$$\Delta E \,=\, 100\,\frac{E_{\mathrm{D1}\alpha\mathrm{T}} \,-\, E_{\mathrm{D1}\alpha}}{E_{\mathrm{D1}\alpha}}\,, \tag{4}$$

which is the relative percentage differences between the binding energies calculated by using interactions with and without tensor term, $E_{\mathrm{D1}\alpha\mathrm{T}}$ and $E_{\mathrm{D1}\alpha}$ respectively ($\alpha \equiv \mathrm{S}, \mathrm{M}$). In this panel the open squares indicate the results obtained with the D1ST and D1S interactions and the solid circles those obtained with the D1MT and D1M ones. The lines have been drawn to guide the eyes.

If we exclude the anomalous values obtained for the ^{14}O nucleus, we observe that all the other results lie in the range $\Delta E \approx \pm 2$. In general, the inclusion of the tensor term in the D1M force produces more binding, while it has opposite effect in the D1S case. These results show that effect of the tensor on the binding energy of the nuclei we have investigated is rather small, confirming the results of Ref. [29]. As a consequence, and as we can see in panels (b) and (c), the inclusion of the tensor term does not modify the agreement with experimental data in a significant manner.

We have investigated the effect of the tensor force on the proton and neutron density distributions obtained from our HF calculations, and, also in this case, we found small effects. We summarize the results of this study in Fig. 4 where we have shown the relative percentage difference between root mean square (rms) radii obtained by using interactions with and without tensor force,

$$\Delta r \,=\, 100\,\frac{\sqrt{\langle r^2\rangle_{\mathrm{D1}\alpha\mathrm{T}}} \,-\, \sqrt{\langle r^2\rangle_{\mathrm{D1}\alpha}}}{\sqrt{\langle r^2\rangle_{\mathrm{D1}\alpha}}}\,. \tag{5}$$

We show the results for the neutron radii in the upper panel of the figure, and those for the proton radii in the lower panel. We have indicated with the open squares the results obtained with the D1S forces and with the solid circles those obtained with the D1M ones.

The effects of the tensor force are rather small, of the order of few parts on a thousand. We observe again the different sign between D1S and D1M results. The larger binding produced by the tensor in the D1M case generates more compact nuclei, i.e. with smaller rms radii. In the case of the D1S forces the effect is just the opposite. This trend is present in both neutron and proton cases.

The results we have presented so far indicate that the bulk properties of the nuclear ground states are not greatly affected by the presence of the tensor force. The situation changes when the s.p. energies are considered. In the remaining part of this section we shall discuss results concerning s.p. properties. Henceforth we shall distinguish the proton and neutron s.p. levels by using the π and ν labels, respectively.

A first quantity we have studied is the difference between the s.p. energies of spin-orbit partner levels

$$s \,=\, \epsilon_{l-1/2} - \epsilon_{l+1/2}\,. \tag{6}$$

In particular, we have studied the difference between the values of s obtained by using forces with and without tensor terms

$$\Delta s \,=\, s_{\mathrm{D1}\alpha\mathrm{T}} \,-\, s_{\mathrm{D1}\alpha}\,. \tag{7}$$

In Figs. 5 and 6 we show the values of Δs calculated for the $1p$, $1d$ and $1f$ proton and neutron levels, respectively, for all the nuclei considered. In these figures the open squares indicate the results obtained with the D1S interactions, and the solid circles those obtained with the D1M ones. The arrows indicate those nuclei where all the spin-orbit partner levels, for both protons and neutrons, are fully occupied.

Let us consider first Fig. 5, where, for each isotope chain we show the evolution of Δs values with the increasing number of neutrons. We first observe that, for each s.p. level investigated, the D1S and D1M results have identical behaviour. Minima and maxima are in the same position for both type of calculations. A second observation is that, in general, Δs is negative. This means that the tensor force reduces the energy difference between spin-orbit partner levels. A third observation is that the effects of the tensor force are minimal, almost zero, for those nuclei indicated with the arrows.

The first observation indicates that the effects we have pointed out are strictly related to peculiarities of the tensor force and of the nucleus investigated. The small difference

between the D1S and D1M results reflects the difference between the tensor forces in D1ST and D1MT, as we have shown in Fig. 1.

The second and third observations are well understood within the scheme proposed by Otsuka *et al.* [9, 10, 41]. The effect of the tensor interaction between a proton and a neutron occupied s.p. levels is attractive if one of the levels has an angular momentum $j_> \equiv l + 1/2$ and the other one $j_< \equiv l - 1/2$. If the angular momenta of the two s.p. levels are of the same type, i.e. both $j_>$ or both $j_<$, the effect of the tensor force has opposite sign. The effect of an occupied neutron level with angular momentum $j_>$ is to increase the energies of the s.p. proton levels with $j_>$, and to lower those of the levels with $j_<$. As a consequence, the splitting between the energies of the proton spin-orbit partner levels is reduced. This effect is reversed when the occupied neutron level has $j_<$. If both $j_>$ and $j_<$ neutron levels are occupied, the two effects cancel with each other.

The results presented in Fig. 5 are well explained within this picture. In the nuclei marked with the arrows, all the $j_>$ and $j_<$ neutron levels are occupied. In these nuclei we do not expect any tensor effect. In reality the values of Δs are not exactly zero even in these cases because we have changed the strengths of the spin-orbit interactions in the forces with tensor terms (see Sec. II). In all the other nuclei there is, at least, one occupied neutron level with $j_>$, whose spin-orbit partner level is empty. The effect we have discussed above predicts negative values of Δs, as those shown in the figure.

In Fig. 6 we have shown the values of Δs for the neutron $1p$, $1d$ and $1f$ levels. Since in the oxygen and calcium isotopes all the proton s.p. partner levels below the Fermi surface are completely occupied, the effects we observe in these isotopes are due to the tensor interaction acting within neutron s.p. levels only. This is exactly the effect we have discussed above, but acting between s.p. states with the same isospin. This effect is weaker than that between states with opposite isospin, as the results for the ^{22}O, ^{24}O, ^{48}Ca and ^{52}Ca nuclei indicate. In these nuclei one of the neutron spin-orbit partner levels is unoccupied and the tensor effect is expected to be present. Actually, there is also an effect produced by the different values of the spin-orbit forces, but we have verified that, for the cases under consideration, this effect is negligible.

The analysis of the Δs results for the Ni, Zr, Sn and Pb isotopes is more complicated, since, in these cases, in both the proton and neutron sectors, there are spin-orbit partner s.p. levels not fully occupied. For this reason, we must consider the interaction with both proton

and neutron levels. The similarity between the behaviour of the results obtained with the different interactions indicate that we are observing an effect due to the peculiarities of the tensor force.

Another quantity of interest related to the s.p. energies is the gap, g, between the energies of the levels just above and just below the Fermi surface. In Fig. 7 we have shown the proton (lower panels) and neutron (upper panels) energy gaps calculated for the nuclei we have investigated with the four forces we are using. Our results are compared with the experimental values (solid triangles) extracted from the binding energies of nuclei with atomic numbers differing by one unit.

The first remark related to the results shown in Fig. 7 is that, in general, the effects of the tensor force are relatively small and they are similar for both type of interactions. They are negligible for neutrons, while some noticeable effects are present in the case of protons. The neutron results, obtained with and without tensor, follow reasonably well the behaviour of the experimental energy gaps.

The effects of the tensor force are better emphasized in Fig. 8 where we show the difference

$$\Delta g \, = \, g_{\mathrm{D1}\alpha\mathrm{T}} \, - \, g_{\mathrm{D1}\alpha} \, , \tag{8}$$

between the gap values obtained by using interactions with and without the tensor force. Also in this case we have indicated with the arrows the nuclei where all the spin-orbit partner levels are fully occupied, for both protons and neutrons. The results obtained with the D1S interactions are shown by the open squares and those obtained with the D1M interactions by the solid circles. It is interesting to observe that also in this case the behaviour of the D1S and D1M results is similar, though the effects produced by the D1ST force are slightly larger than those obtained for D1MT.

Also the results in Fig. 8 can be well explained within the scheme proposed by Otsuka. In the spin unsaturated oxygen isotopes, the unpaired neutron levels are always of $j_>$ type. The tensor force lowers the energy of the $(1p_{1/2})_\pi$ occupied proton level ($j_<$ type) and increases that of the $(1d_{5/2})_\pi$ empty level ($j_>$ type). For this reason, the results for the oxygen isotopes, in the proton case, have positive values. An analogous effect is present also for the ^{48}Ca and ^{52}Ca isotopes. In this case, the states to be considered are the holes $(1d_{3/2})_\pi$ or $(2s_{1/2})_\pi$ and the particle $(1f_{7/2})_\pi$.

For the heavier isotopes, the situation is more complicated because the unpaired levels

can be more than one, and because the levels involved in the gap calculation could be both of the same type ($j_>$ or $j_<$). This is the case for Z or N=28 or 50, but not for $Z = 40$. For this reason, in the case of protons, the values of Δg are negative for Ni, Sn and Pb isotopes and positive for ^{90}Zr.

For the neutrons, panel (a), the situation is more difficult to discuss since the nuclei we have investigated are not isotones. For each set of isotopes there are different s.p. levels related to the neutron gap, therefore the effect of the tensor term can be different for each nucleus considered. This is the reason of the oscillating behaviour we observe in the Ni isotopes.

Since oxygen and calcium isotopes are spin saturated in protons, the results presented in the panel (a) of Fig. 8 for these nuclei, are produced by the interaction of an unpaired neutron s.p. level of $j_>$ type with the neutron s.p. levels just below and above the Fermi surface. The comparison of the results of these nuclei shown in the two panels indicates that the effect of the tensor interaction between like nucleons is smaller than that between neutrons and protons, reflecting the fact that we have used a tensor-isospin term in the interaction.

We have seen that the tensor term affects more the s.p. than the bulk properties of the nucleus. The effects of the tensor force on the s.p. levels can modify their relative order. If this occurs for the levels near the Fermi surface, the spin of even-odd nuclei neighboring the nuclei investigated, which is determined by the last unpaired nucleon, should be modified. We found some cases where this happens and few of them are presented in Fig. 9, where we show the evolution of the states near the Fermi surface for the different interactions we have used.

In the ^{48}Ca case we consider the two proton states below the Fermi surface. The $(1d_{3/2})_\pi$ is a $j_<$ state, therefore its energy is lowered by the tensor, while that of the $(2s_{1/2})_\pi$ state remains essentially unchanged. This effect inverts the order of the two states, as we observe in the results of the D1ST column. The calculations done with the D1M interaction give the two proton states in an inverted order with respect to that of the D1S one. In this case the tensor effect enlarges the energy difference between the two states. Since ^{48}Ca and ^{48}Ni are mirror nuclei, we expected an analogous effect for the two neutron hole states in ^{48}Ni. This effect is present in our calculations as it is shown in the figure.

Since all the spin-orbit partner levels are occupied for both protons and neutrons, we do

not expect tensor effects in ^{60}Ca. This is what we observe in Fig. 9. We show the results for this nucleus since the order of the proton hole states obtained with the D1S and D1ST interactions is inverted with respect to that obtained with the D1M and D1MT forces.

In the ^{78}Ni case, the tensor force produces a large lowering of the $(1f_{5/2})_\pi$ level, and this, for the D1M interaction, generates an inversion with the $(2p_{3/2})_\pi$ level. The figure shows that the tensor force reduces the energy gap between $(1f_{5/2})_\pi$ and $(1f_{7/2})_\pi$ levels.

For the ^{100}Sn nucleus we show both proton and neutron cases, since in both situations we obtain the inversion of the $1g_{7/2}$ and $2d_{5/2}$ levels, when the D1ST interaction is used. The tensor force lowers the energies of the $1g_{7/2}$ levels, which are $j_<$ states, and enhances those of the $2d_{5/2}$ levels, which are $j_>$ states. We obtain a large effect on the energies of the $1g_{7/2}$ levels while the modification of the $2d_{5/2}$ energy is minimal.

We observe an inversion of the order of the $(2d_{3/2})_\nu$ and $(3s_{1/2})_\nu$ levels in ^{114}Sn, when the D1ST interaction is used. The tensor lowers the energy of the $(2d_{3/2})_\nu$ state, of $j_<$ type, and has no effect on the $(3s_{1/2})_\nu$ state. The effect is present also when the D1MT interaction is used, but it is not large enough to invert the order of the states.

In ^{116}Sn we obtain an inversion of the order of the $(1g_{7/2})_\pi$ and $(2d_{3/2})_\pi$ levels when both D1ST and D1MT interactions are used. Also in this case we observe the tensor effect predicted by the Otsuka's scheme. The energy of the $(1g_{7/2})_\pi$ state, of $j_<$ type, is lowered, while that of the $(2d_{3/2})_\pi$ state, of $j_>$ type, is enhanced.

To summarize the results presented in this section, we may say that the tensor effects have remarkable consequences on those observables which we relate to s.p. properties of the nuclear system, such as s.p. energies, gaps and spin of the system.

IV. RPA CALCULATIONS

In the previous section we have presented the results regarding the ground state properties of some spherical nuclei. In this section we show the results we have obtained for the excited states of these nuclei by doing RPA calculations. In this study, we have also considered ^{12}C, a well studied nucleus from both experimental and theoretical points of view, despite the fact that its ground state contains deformations [38]. This feature is less important in the description of the excitation spectrum than for the ground state observables.

The input required by any RPA calculations is composed by the s.p. basis and the

effective interaction. The results shown in this section have been obtained by using the s.p. basis and the effective interaction provided by HF calculations. In the RPA jargon this procedure is called self-consistent to distinguish it from the phenomenological one described in Sec. I. To be precise, we do not strictly use the same interaction in HF and RPA, since in the latter case we neglect the Coulomb and spin-orbit terms of the interaction. We should keep in mind this fact, even though there are indications that, in RPA calculations, these two terms of the interaction produce very small effects that, in addition, have the tendency of canceling with each other [42].

The strategy of our investigation is analogous to that used in the previous section, i.e. we compare results obtained by using interactions with and without tensor terms. While for the HF calculations this comparison provides a clear indication of the effects of the tensor force, in the RPA case the situation is more complicated. In effect, the differences in the RPA results can be due to genuine effects of the tensor interaction in the RPA calculations, and also to the different values of the s.p. energies and wave functions provided by the HF results.

We have disentangled the effects produced by these two different sources by presenting results where the tensor force is switched on and off in both HF and RPA calculations. To distinguish the results of the different type of calculations we have indicated with $\omega_{\rm ab}^{\rm RPA}$ the RPA excitation energies, where the first subindex, a, refers to the interaction used in the HF calculation, and the second subindex, b, to that used in the RPA one. The a and b labels can be t if the interaction includes the tensor term, i.e. if the D1ST or the D1MT interaction has been used, and n otherwise. For example, $\omega_{\rm nt}^{\rm RPA}$ indicates the excitation energy obtained with a HF calculation without tensor and a RPA calculation with the tensor force. We present also results obtained by switching off the residual interaction. We label these results as $\omega_{\rm a}^{\rm IPM}$, where the superscript IPM means Independent Particle Model. The energies produced in this type of calculations need only one subindex which indicates the presence, t, or the absence, n, of the tensor force in the HF calculation.

In our study we have investigated various types of multipole excitations, and, in agreement with the results of Refs. [15, 21, 25], we found that the natural parity excitations are practically insensitive to the effects of the tensor force. For this reason, we present here only results obtained for the unnatural parity excitations.

We start or discussion by presenting the results related to the excitation of the first 0^-

state in the various isotopes we are studying. In the phenomenological calculations of Sec. II we have pointed out the large sensitivity of the excitation energy of these states to the tensor force. For this reason we have chosen the energy of this excitation in ^{16}O to select the strengths of our tensor forces.

For the nuclei where the 0^- excitation energies have been experimentally clearly identified [26, 27], we show in Table I the excitation energies obtained in our RPA calculations. The tensor interaction lowers the excitation energies in all the cases. The perfect agreement of the ^{16}O case is obtained by construction, but we have improvements also in the ^{40}Ca, ^{48}Ca and ^{208}Pb cases. The only worsening produced by the inclusion of the tensor term is that of the ^{12}C nucleus, which we know to be a difficult nucleus to describe within our theoretical framework tailored to spherical systems.

A general view of the tensor effects in all the nuclei we have considered is given in Fig. 10. In panel (a) we show the differences $\omega_{\rm tt}^{\rm RPA} - \omega_{\rm nn}^{\rm RPA}$ for the first 0^- states in all the nuclei under investigation. The open squares show the results for the interactions of D1S type, while the solid circles those of the D1M one. To separate the tensor effects in RPA calculations from those produced by the change in the s.p. configuration space, we show in panel (b) the energy differences $\omega_{\rm t}^{\rm IPM} - \omega_{\rm n}^{\rm IPM}$.

In the RPA calculations, the results obtained with the tensor force are always lower than those obtained without it, and this produces negative values of the differences $\omega_{\rm tt}^{\rm RPA} - \omega_{\rm nn}^{\rm RPA}$. The only exception to this general trend is that of the ^{14}O nucleus in the case of the D1M interaction. In reality we observe in panel (b) that the differences $\omega_{\rm t}^{\rm IPM} - \omega_{\rm n}^{\rm IPM}$ for this nucleus are positive and larger than those found in the RPA calculation, indicating that also in this case the tensor force in the RPA calculation lowers the energy value of the first 0^- state.

The results presented in the two panels do not show any correlation. This indicates that the effect shown in the panel (a) of the figure is a genuine effect of the tensor force on the RPA calculations, which, in the case of the 0^- excitation, is always attractive, even in the ^{14}O case, confirming the results we have obtained with the phenomenological calculations and shown in Fig. 2.

We have investigated the effects of the tensor force on multipole excitations with strong isoscalar (IS) or isovector (IV) character. To identify well these states we have considered only isotopes with $N = Z$. In these nuclei, we have selected those multipole excitations com-

posed mainly by two identical particle-hole pairs in terms of angular momentum coupling, but one for protons and the other one for neutrons. This is the ideal situation to produce IS and IV partners levels. In the first case proton and neutron excitations are in phase, while in the second one are off phase. In our RPA results the IS and IV partner states are easily identifiable by observing the relative phases of the RPA amplitudes of the main particle-hole pairs.

We have presented in Table II the energies of the excited states we have investigated, and we compare them with the available experimental values [43]. All the results indicate that the energies of the IV excitations are larger than those of the IS ones, as it is experimentally well established. In Ref. [24] we obtained for the calculations done with the D1S interaction an opposite behaviour. These results were wrong, since we found an error in the treatment of the exchange part of the density dependent terms of the D1S force.

The effects of the tensor terms are better presented in Fig. 11. In the panels (a) and (b) we show the energy differences $\omega_{\rm tt}^{\rm RPA} - \omega_{\rm nn}^{\rm RPA}$ for IS (open squares) and IV (solid circles) states. The results found for the various calculations have rather similar behaviours. The tensor effects are smaller on the IV states. In the panels (c) and (d) we show the differences between the energies of the IV and IS states for each multipole we have considered. In these panels the open squares show the results obtained without tensor interaction, while the solid circles include the tensor in both HF and RPA calculations. The tensor force always increases these differences. In general, this enhancement is larger for D1S than for D1M and it is worth pointing out that the effect is relatively large for the three 1^+ states studied (in ^{12}C and ^{56}Ni and ^{100}Sn) in case of the D1S interaction.

We have studied the effects of the tensor force on the electron scattering responses. A detailed presentation of these results would require a discussion for each specific excited state. We plan to make this discussion in the future. At the moment we can summarize the main and general feature we have observed by saying that the effects of the tensor force are larger on the IS excitations than on the IV ones. As example, we show in Fig. 12 the inclusive inelastic electron scattering transverse responses [44] as a function of the effective momentum transfer, for the 1^+ isospin excitation doublet in ^{12}C, and the 2^- doublet in ^{40}Ca, and we compare them with the available experimental data [45, 46]. It is evident that the effects of the tensor are greater on the IS than on the IV excited states.

The explanation of these facts is related to the structure of the electromagnetic excitation

of the unnatural parity states, which is dominated by the magnetization current [44]. The magnetization current depends on the anomalous magnetic moment of the nucleon, which has different sign for protons and neutrons. Since in the IS excitations the main proton and neutron RPA amplitudes have the same sign, the proton and neutron magnetization currents subtract with each other. In the IV excitations the effect is reversed. Small differences in the proton and neutron structure of the RPA wavefunctions are emphasized by the difference and hidden in the sum of the proton and neutron contributions.

A remarkable sensitivity to the tensor force of the 1^+ excitation of ^{48}Ca has been pointed out in Ref. [15]. The two tensor forces used together with the Skyrme interactions in that article produce opposite results. We have investigated how our tensor forces affects the energy of the first 1^+ excitation in the nuclei with different number of protons and neutrons we have considered. We have summarized in Fig. 13 our results. In this figure we show the differences between the 1^+ excitation energies obtained in different type of calculations. The states selected are those with the largest B-value and all of them are dominated by a neutron p-h configuration. Solid circles indicate the energy differences $\omega_{\rm t}^{\rm IPM} - \omega_{\rm n}^{\rm IPM}$. With the black squares we have shown the energy differences $\omega_{\rm tt}^{\rm RPA} - \omega_{\rm tn}^{\rm RPA}$ indicating the effect of the tensor forces in the RPA calculation. Finally, the open squares show the energy differences $\omega_{\rm tt}^{\rm RPA} - \omega_{\rm nn}^{\rm RPA}$, which are linked to the global effect of the tensor in our self-consistent calculations.

The results shown in the figure indicate that the presence of the tensor force changes the s.p. energies in a way that the energy of the excitation is reduced. This is shown by the fact that all the energy differences have negative sign. These results are in agreement with the findings of Cao *et al.* [15] for the T44 interaction [16] and they have opposite behaviour of those found by the same authors for the modified SLy5 interaction [14]. In their calculations this is due to the change of the overall sign of the tensor term for the N-N pairs with the same isospin ($\pi\pi$ or $\nu\nu$ pairs).

As we have observed in all the results presented so far, the tensor effects are smaller for the D1M interaction. The effect of the tensor force is almost zero for the two nuclei where all the s.p. spin-orbit partner levels are occupied, i.e. ^{28}O and ^{60}Ca. With the exception of these two cases, the differences $\omega_{\rm tt}^{\rm RPA} - \omega_{\rm nn}^{\rm RPA}$ are noticeably larger than $\omega_{\rm t}^{\rm IPM} - \omega_{\rm n}^{\rm IPM}$.

To investigate the effect of the tensor force in RPA, we have calculated the energy differences $\omega_{\rm tt}^{\rm RPA} - \omega_{\rm tn}^{\rm RPA}$ where the same s.p. basis is used for the two RPA calculations. These

results are presented in Fig. 13 by solid squares. We added incoherently the $\omega_{\rm t}^{\rm IPM} - \omega_{\rm n}^{\rm IPM}$ and the $\omega_{\rm tt}^{\rm RPA} - \omega_{\rm tn}^{\rm RPA}$ results and we obtained the results plotted with crosses which reproduce very well the results of the complete calculation $\omega_{\rm tt}^{\rm RPA} - \omega_{\rm nn}^{\rm RPA}$. These results validate the assumption used by Cao *et al.* in Ref. [15].

We conclude this section by presenting the results obtained for the 1^+ excitation of ^{208}Pb which has attracted great attention in the past [47–50], and whose interest has been renewed by recent measurements [51]. Energies and B-values for the first two 1^+ excited states obtained with the four interactions are shown in Table III. We observe that the tensor lowers the values of the energies of both states. The $B(M1)$ value of the first state is lowered by the tensor force, while that of the second excited state, which is the state included in Fig. 13, is increased.

The detailed analysis of the results shows that the effects of the tensor force on the energy values improve the agreement with the experimental values. The situation regarding the $B(M1)$ values is more complex. The tensor force lowers the $B(M1)$ values of the first state, and this improves the agreement with the experiment. The situation is reversed for the second excited state. Our results are compatible with those found in literature [21, 25, 47, 51]. The large difference between the theoretical and experimental $B(M1)$ values of the second state can be attributed to the limitations of the RPA which is unable to describe the large fragmentation of the second 1^+ state.

We show in Fig. 14 the inelastic electron scattering responses [44], calculated for these two states and we compare them with the data of Ref. [48]. We observe that there is a larger sensitivity to the tensor force in the case of the first excited state.

V. SUMMARY AND CONCLUSIONS

We have studied the effects of the tensor terms of interactions used in HF and RPA theories. We considered only finite-range terms in the tensor-isospin channel, because they are the most important terms in microscopic interactions. We constructed these tensor terms by multiplying the analogous term of the microscopic Argonne V18 interaction by a function which modifies its behaviour at short internucleonic distances. This function contains a single parameter whose value determines the strength of the tensor force.

To determine this strength, we searched for a global observable particularly sensitive

to the tensor force, and, by using phenomenological RPA calculations, we found it in the excitation of the 0^- states. We have also observed that the tensor force strongly influences the values of the s.p. energies. We constructed new effective interactions by adding a tensor-isospin term to finite range interactions, and we selected the strength of the tensor and spin-orbit forces to reproduce, in the ^{16}O nucleus, the experimental energy of the first 0^- excited state, and the splitting between the s.p. energies of the neutron $1p_{3/2}$ and $1p_{3/2}$ levels. We based our work on the D1S and D1M parameterizations of the Gogny interaction, and we called D1ST and D1MT the two new effective interactions constructed with a recursive procedure where HF and RPA calculations have been repeated until both experimental quantities have been reproduced.

The study of the effects of these tensor forces has been done by comparing the results obtained in HF and RPA calculations, using interactions with and without tensor terms. We have repeated each calculation with both D1S and D1M type of effective interactions to extract genuine tensor effects from those related to the peculiarities of a specific choice of the force parameters. We always found great similarities between the results obtained with the two different type of parameterizations. Since the strength of the tensor force in D1MT is weaker than that of D1ST, we found smaller tensor effects in the results obtained with D1MT than in those for D1ST. We have done calculations for a set of spherical nuclei chosen such as all the s.p. levels below the Fermi surface are fully occupied. With this choice we avoided the effects of the deformation and we minimized those of the pairing.

Our HF calculations indicate that tensor forces do not produce sensitive effects on bulk observables such as binding energies, radii and density distributions. The effects of the tensor force on quantities related to the s.p. properties of our theoretical approach are certainly more remarkable. We have calculated energy splitting between spin-orbit partner levels, energy gaps between the s.p. states just above and below the Fermi surface, and we found noticeable effects produced by the tensor force. Also the ordering of the s.p. levels around the Fermi surface, which determines the spin of the even odd nuclei neighboring those we have studied, is strongly influenced by the presence of the tensor force in some cases. We could explain all our results within the picture proposed by Otsuka and collaborators [9, 10], eventually by extending it to consider the interaction between nucleons of the same type.

The study of tensor effects in the excitation spectra is more complex, since the effects of the tensor force in the RPA calculations add to those already present in the HF calculation

that produces the s.p. bases. In our investigation we have disentangled the effects coming from these two different sources.

We have verified the well know fact [21, 25] that natural parity excitations are essentially unaffected by the tensor force. For this reason we have presented results regarding unnatural parity excitations only. We started our investigation by studying the 0^- excitations in various nuclei, and we found that the excitation energies obtained with the tensor forces are always smaller than those obtained without it.

We studied the different role played by the tensor force in IS and IV type of excitations. To identify clearly these different type of excitation modes, we have considered nuclei with equal number of protons and neutrons, and states dominated by particle-hole transitions with the same angular momentum coupling for both protons and neutrons. The energies of the IV modes are always greater than those of the IS modes with or without tensor. These results agree with the experimental observations. We found that the IS excitations are more sensitive to the tensor force than the IV ones. The tensor force increases the energy difference between IS and IV excitations.

We made a systematic study of the effects of the tensor force on the excitation of the 1^+ states in nuclei with different number of protons and neutrons. We have considered the states showing the largest $B(M1)$-values, and we found that the tensor force consistently lowers the values of their excitation energies. This is essentially obtained as the incoherent sum of the effect generated by the HF calculation and that obtained by the RPA.

The study of the excitation of the first two 1^+ excited states in ^{208}Pb indicates that the lower energy state is more sensitive to the tensor force than the other one. The presence of the tensor force modifies energies and $B(M1)$-values, and slightly improves the agreement with the experimental data [51], even though the limitations of the RPA theory do not allow a description of the fragmentation of the strength of the higher energy state.

We have restricted our study to charge conserving nuclear excitations. There are indications that the effects of the tensor-isospin force are more relevant on the charge-exchange excitations [52–54]. The presence of the tensor forces seems to be relevant also in the description of the reactions between heavy nuclei [55].

We think that the accuracy required today by self-consistent effective theories requires the use of interactions containing tensor terms.

Acknowledgments

This work has been partially supported by the Spanish Ministerio de Ciencia e Innovación under contracts FPA2009-14091-C02-02 and ACI2009-1007 and by the Junta de Andalucía (FQM0220).

[1] J. Kellog, I. Rabi, N. Ramnsey, J. Zacharias, Phys. Rev. 57 (1939) 677.

[2] A. Nordsieck, Phys. Rev. 58 (1940) 310.

[3] W. Rarita, J. Schwinger, Phys. Rev. 59 (1941) 436.

[4] W. Rarita, J. Schwinger, Phys. Rev. 59 (1941) 556.

[5] A. Ozawa, T. Kobayashi, T. Suzuki, K. Yoshida, T. Tanihata, Phys. Rev. Lett. 84 (2000) 5493.

[6] R. Kanungo, I. Tanihata, A. Ozawa, Phys. Lett. B 528 (2002) 58.

[7] J. P. Schiffer, et. al., Phys. Rev. Lett. 92 (2004) 162501.

[8] O. Sorlin, M.-G. Porquet, Prog. Part. Nucl. Phys. 61 (2008) 602.

[9] T. Otsuka, T. Suzuki, R. Fujimoro, H. Grawe, Y. Akaishi, Phys. Rev. Lett. 95 (2005) 232502.

[10] T. Otsuka, T. Matsuo, D. Abe, Phys. Rev. Lett. 97 (2006) 162501.

[11] D. M. Brink, F. Stancu, Phys. Rev. C 75 (2007) 064311.

[12] S. Sugimoto, H. Toki, K. Ikeda, Phys. Rev. C 76 (2007) 054310.

[13] D. Tarpanov, H. Liang, N. Van Giai, C. Stoyanov, Phys. Rev. C 77 (2008) 054316.

[14] G. Colò, H. Sagawa, S. Fracasso, P. F. Bortignon, Phys. Lett. B 646 (2007) 227.

[15] L.-G. Cao, G. Colò, H. Sagawa, P. F. Bortignon, L. Sciacchitano, Phys. Rev. C 80 (2009) 064304.

[16] T. Lesinski, M. Bender, K. Bennaceur, T. Duguet, J. Meyer, Phys. Rev. C 76 (2007) 014312.

[17] R. Machleidt, K. Holinde, C. Elster, Phys. Rep. 149 (1987) 1.

[18] R. B. Wiringa, V. G. J. Stoks, R. Schiavilla, Phys. Rev. C 51 (1995) 38.

[19] F. Arias de Saavedra, C. Bisconti, G. Co', A. Fabrocini, Phys. Rep. 450 (2007) 1.

[20] J. Speth, E. Werner, W. Wild, Phys. Rep. 33 (1977) 127.

[21] J. Speth, V. Klemt, J. Wambach, G. E. Brown, Nucl. Phys. A 343 (1980) 382.

[22] A. Migdal, Theory of finite Fermi systems and applications to atomic nuclei, Interscience, London, 1967.

[23] G. Co', V. De Donno, C. Maieron, M. Anguiano, A. M. Lallena, Phys. Rev. C 80 (2009) 014308.

[24] V. De Donno, G. Co', C. Maieron, M. Anguiano, A. M. Lallena, M. Moreno-Torres, Phys. Rev. C 79 (2009) 044311.

[25] G. Co', A. M. Lallena, Nucl. Phys. A 510 (1990) 139.

[26] Brookhaven National Laboratory, National nuclear data center, http://www.nndc.bnl.gov/.

[27] A. Heusler, G. Graw, R. Hertenberger, F. Riess, H.-F. Wirth, R. Krücken, P. von Brentano, Phys. Rev. C 75 (2007) 024312.

[28] A. R. Bautista, G. Co', A. M. Lallena, Nuov. Cim. A 112 (1999) 1117.

[29] G. Co', A. M. Lallena, Nuov. Cim. A 111 (1998) 527.

[30] R. Guardiola, J. Ros, J. Comp. Phys. 45 (1982) 374.

[31] R. Guardiola, H. Schneider, J. Ros, Anales de Fìsica 78 (1982) 154.

[32] V. De Donno, Nuclear excited states within the random phase approximation theory, Ph.D. thesis, Università del Salento (Italy), http://www.fisica.unisalento.it/ gpco/stud.html (2008).

[33] V. De Donno, G. Co', M. Anguiano, A. M. Lallena, arXiv:1011.5088 [nucl-th].

[34] J. F. Berger, M. Girod, D. Gogny, Comp. Phys. Commun. 63 (1991) 365.

[35] S. Goriely, S. Hilaire, M. Girod, S. Péru, Phys. Rev. Lett. 102 (2009) 242501.

[36] J. Dechargè, D. Gogny, Phys. Rev. C 21 (1980) 1568.

[37] H. Nakada, Phys. Rev. C 68 (2003) 014316.

[38] J.-P. Delaroche, M. Girod, J. Libert, H. Goutte, S. Hilaire, S. Péru, N. Pillet, G. F. Bertsch, Phys. Rev. C 81 (2010) 014303.

[39] G. Audi, A. H. Wapstra, C. Thibault, Nucl. Phys. A 729 (2003) 337.

[40] http://ie.lbl.gov/toi2003/masssearch.asp.

[41] T. Otsuka, T. Suzuki, Y. Utsuno, Nucl. Phys. A 805 (2008) 127c.

[42] T. Sil, S. Shlomo, B. K. Agrawal, P. G. Reinhard, Phys. Rev. C 73 (2006) 034316.

[43] C. M. Lederer, V. S. Shirley, Table of isotopes, 7th ed., John Wiley and sons, New York, 1978.

[44] J. Heisenberg, H. Blok, Ann. Rev. Nucl. Par. Sci. 33 (1983) 569.

[45] Hyde-Wright, Particle-hole structure in ^{16}O, Ph.D. thesis, Massachusetts Institute of Technology, unpublished (1984).

[46] C. F. Williamson, et al., unpublished (1987).

[47] R. M. Laszewski, J. Wambach, Comments Nucl. Part. Phys. 14 (1985) 321.

[48] S. Müller, G. Küchler, A. Richter, H. P. Blok, H. Blok, C. W. de Jager, H. de Vries, J. Wambach, Phys. Rev. Lett. 54 (1985) 293.

[49] J. L. Tain, G. P. A. Berg, I. Katayama, S. A. Martin, J. Meissburger, J. G. M. Römer, J. Wambach, Phys. Rev. C 35 (1987) 1288.

[50] R. M. Laszewski, R. Alarcon, D. S. Dale, S. D. Hoblit, Phys. Rev. Lett. 61 (1988) 1710.

[51] T. Shizuma, et al., Phys. Rev. C 78 (2009) 061303(R).

[52] C. L. Bai, H. Sagawa, H. Q. Zhang, X. Z. Zhang, G. Colò, F. R. Xu, Phys. Lett. B 675 (2009) 28.

[53] C. L. Bai, H. Q. Zhang, X. Z. Zhang, F. R. Xu, H. Sagawa, G. Colò, Phys. Rev. C 79 (2009) 041301(R).

[54] C. L. Bai, H. Q. Zhang, H. Sagawa, X. Z. Zhang, G. Colò, F. R. Xu, Phys. Rev. Lett. 105 (2010) 072501.

[55] Y. Iwata, J. A. Marhun, arXiv:1012.3363 [nucl-th].

	exp	D1S	D1ST	D1M	D1MT
^{12}C	18.40	19.63	14.42	18.83	15.27
^{16}O	10.96	13.95	10.94	13.08	10.96
^{40}Ca	10.78	12.22	9.57	11.56	9.60
^{48}Ca	8.05	14.10	11.63	12.85	11.26
^{208}Pb	5.28	8.27	7.93	8.24	7.92

Table I: Energies, in MeV, of the first 0^- excited state for those isotopes we have studied in this work where the energy values have been measured [26, 27]. The theoretical energies are obtained by doing RPA calculations with different interactions.

		D1S		D1ST		D1M		D1MT		exp	
	J^π	IS	IV	IS	IV	IS	IV	IS	IV	IS	IV
^{12}C	1^+	4.78	7.71	1.94	8.17	3.44	7.21	2.43	7.68	12.71	15.11
^{12}C	2^-	15.75	18.62	14.27	17.30	14.59	18.06	13.50	17.15	11.83	13.35
^{12}C	4^-	17.11	18.35	15.61	17.08	16.22	17.40	15.18	16.61	18.27	19.50
^{16}O	2^-	10.36	12.10	9.64	12.08	9.47	11.26	8.74	11.08	8.87	12.53
^{16}O	4^-	17.08	18.20	16.52	17.96	16.02	16.97	15.63	16.86	17.79	18.98
^{40}Ca	2^-	7.61	8.98	6.62	8.83	6.63	8.31	5.82	8.01	7.53	8.42
^{40}Ca	4^-	6.93	7.51	6.37	7.41	6.68	7.04	6.02	6.70	5.61	7.66
^{40}Ca	6^-	14.48	15.15	14.15	14.95	13.66	14.17	13.44	14.07		
^{56}Ni	2^-	11.64	14.32	11.06	13.91	11.10	13.50	10.62	13.35		
^{56}Ni	4^-	12.57	13.60	11.98	13.08	12.01	12.93	11.58	12.56		
^{56}Ni	5^+	6.73	7.13	4.86	5.37	6.00	6.29	5.00	5.52		
^{100}Sn	3^+	8.70	8.97	5.56	6.38	8.09	8.21	6.37	6.68		
^{100}Sn	5^+	7.10	7.39	5.53	6.29	6.66	6.88	5.97	6.22		
^{100}Sn	7^+	7.30	7.56	5.44	6.18	7.91	8.05	6.03	6.38		

Table II: Excitation energies, in MeV, in nuclei with $Z = N$, for different multipoles, where we have identified isoscalar (IS) and isovector (IV) character. The experimental values are taken from Ref.[43].

	exp	D1S	D1ST	D1M	D1MT
$E(1_1^+)$ [MeV]	5.85	7.80	4.76	6.50	4.82
$B(M1)_1$ $[\mu^2_n]$	2.0	5.08	2.41	2.33	1.80
$E(1_2^+)$ [MeV]	7.1-8.7	10.15	8.06	9.42	8.38
$B(M1)_2$ $[\mu^2_n]$	16.0 (17.9)	29.63	32.84	31.46	32.26

Table III: Energies and $B(M1)$ values, expressed in terms of nuclear magnetons, of the first two 1^+ excitations in ^{208}Pb obtained by using different interactions. The experimental values are taken from Ref. [51].

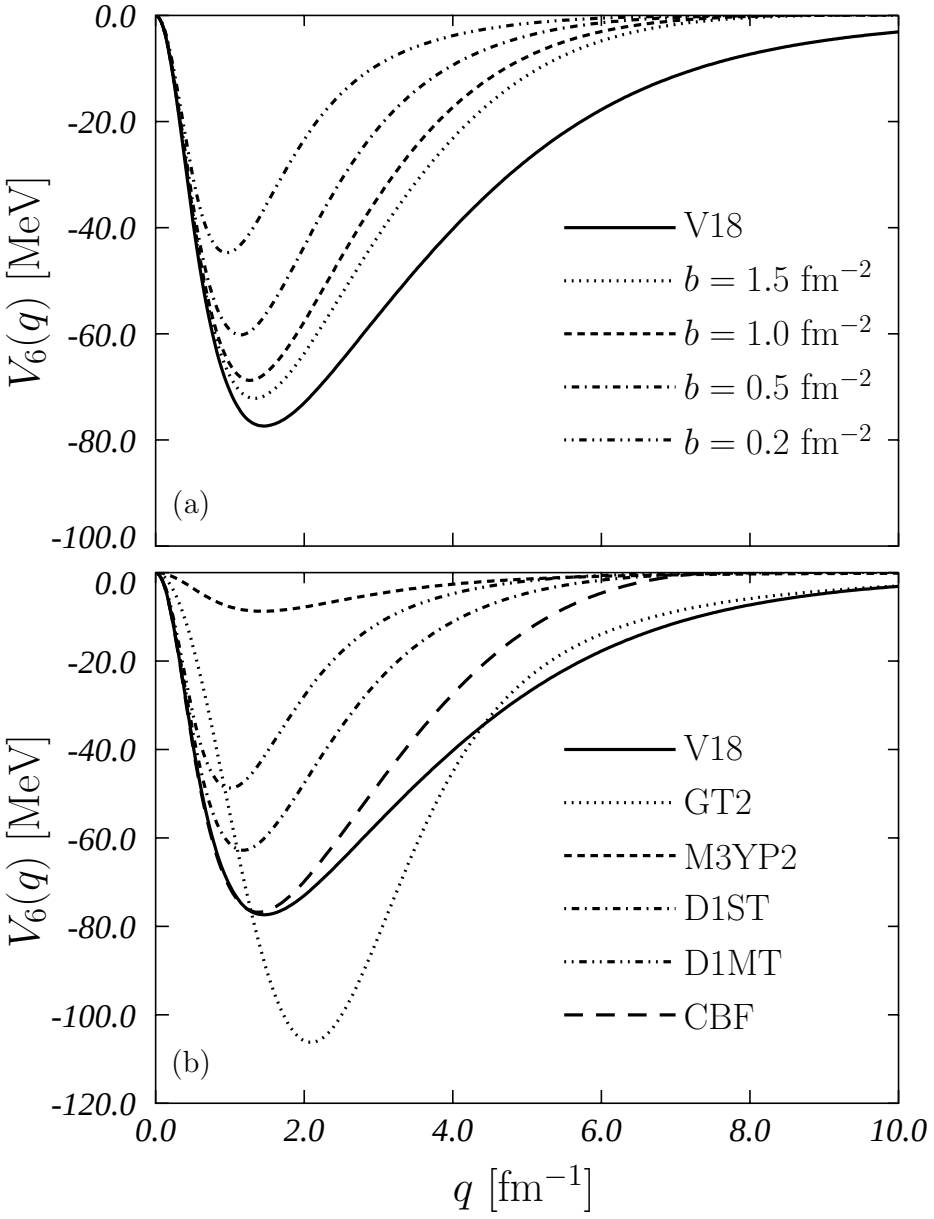

Figure 1: Momentum dependent term of the tensor force, see Eq. (2), for various parameterizations. In the panel (a) we compare the tensor-isospin term of the bare Argonne V18 interaction (full line) with the interactions obtained from Eq. (1) by using different values of the parameter b. In panel (b) we compare the bare Argonne V18 term with the tensor term of the GT2 force of Ref. [10] (dotted line) and with that of the M3YP2 force of Ref. [37] (short-dashed line). The tensor forces we have constructed, named D1ST and D1MT, are indicated by the dashed-dotted and dashed-doubly-dotted lines. The long-dashed line (CBF) shows the tensor term obtained by multiplying the bare Argonne V18 interaction with the scalar part of the correlation function obtained in microscopic Correlated Basis Function calculations [19].

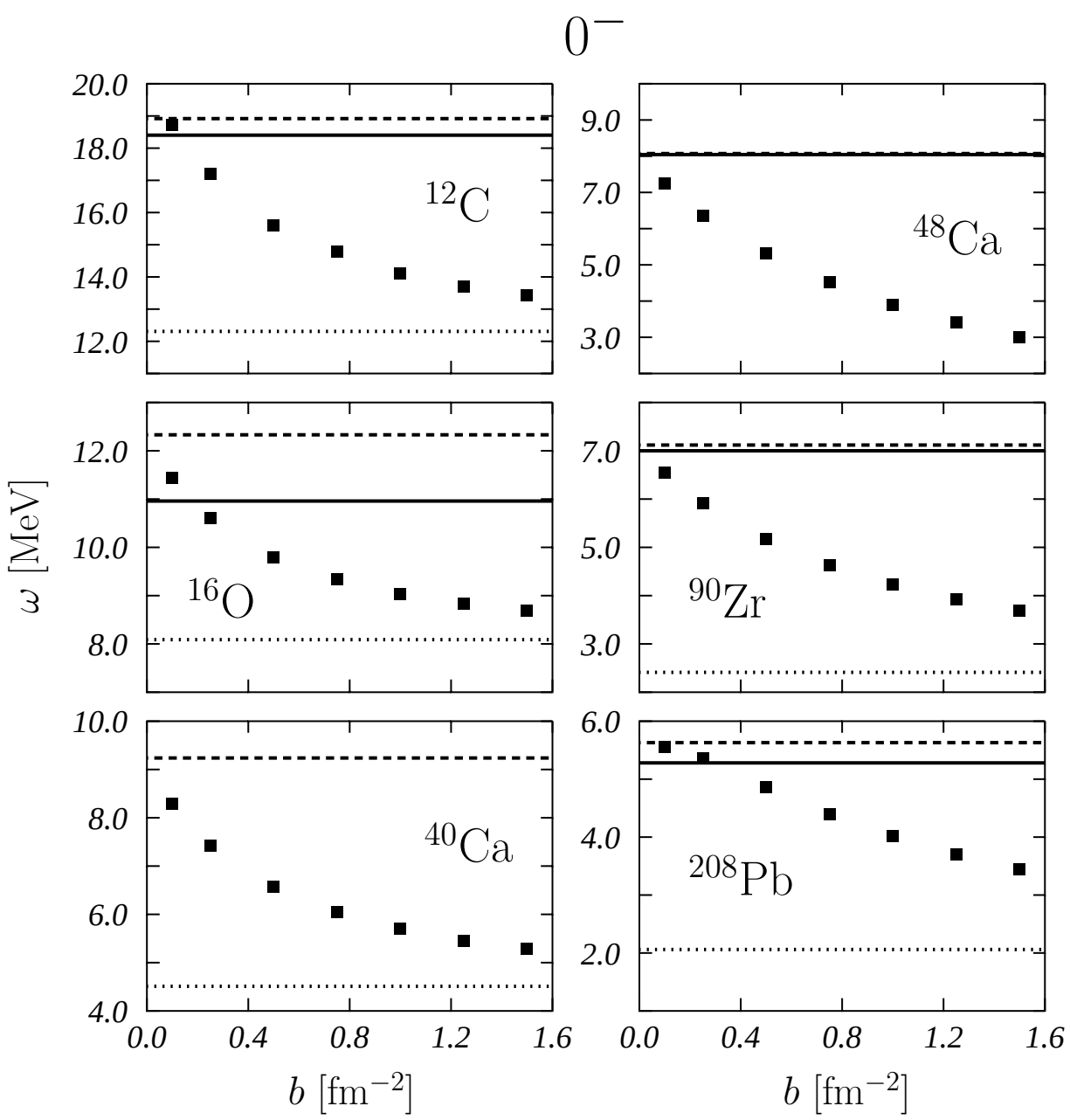

Figure 2: The squares show the values of the excitation energies of the lowest 0^- states for various nuclei as a function of the value of the parameter b of Eq. (1) ruling the strength of the tensor force. The full lines show the experimental values, the dashed lines the values obtained without tensor, and the dotted lines the values obtained with the full tensor term of the Argonne V18 interaction.

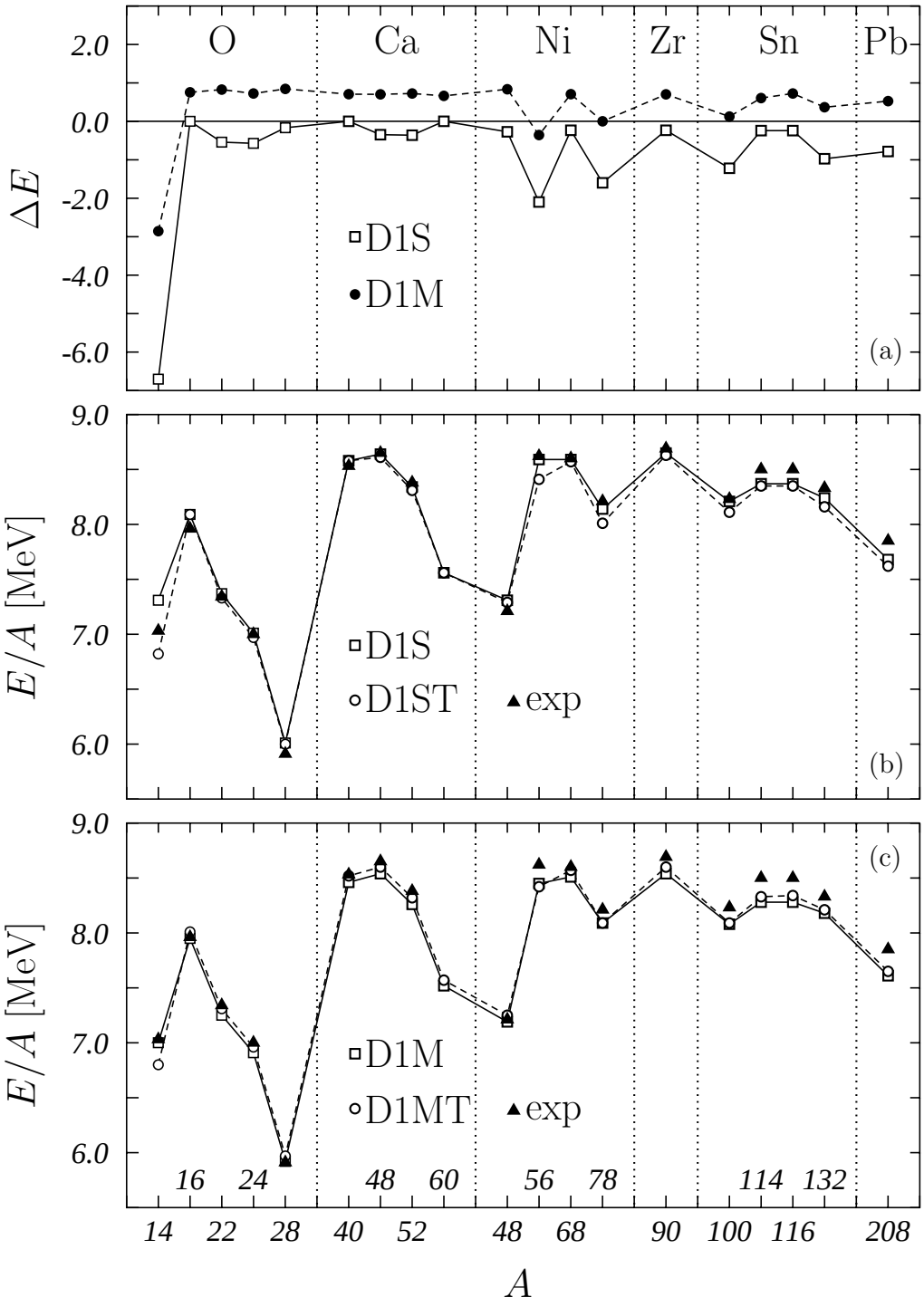

Figure 3: Panel(a): relative percentage differences, Eq. (4), between binding energies calculated with the D1ST and D1S forces (open squares) and with the D1MT and D1M (solid circles) interactions. Panels (b) and (c): binding energies per nucleon calculated with the various interactions compared with the experimental values (solid triangles) taken from Ref. [39, 40]. The experimental values for the ^{28}O, ^{60}Ca, ^{48}Ni, ^{78}Ni and ^{100}Sn nuclei are estimated [40]. The lines have been drawn to guide the eyes.

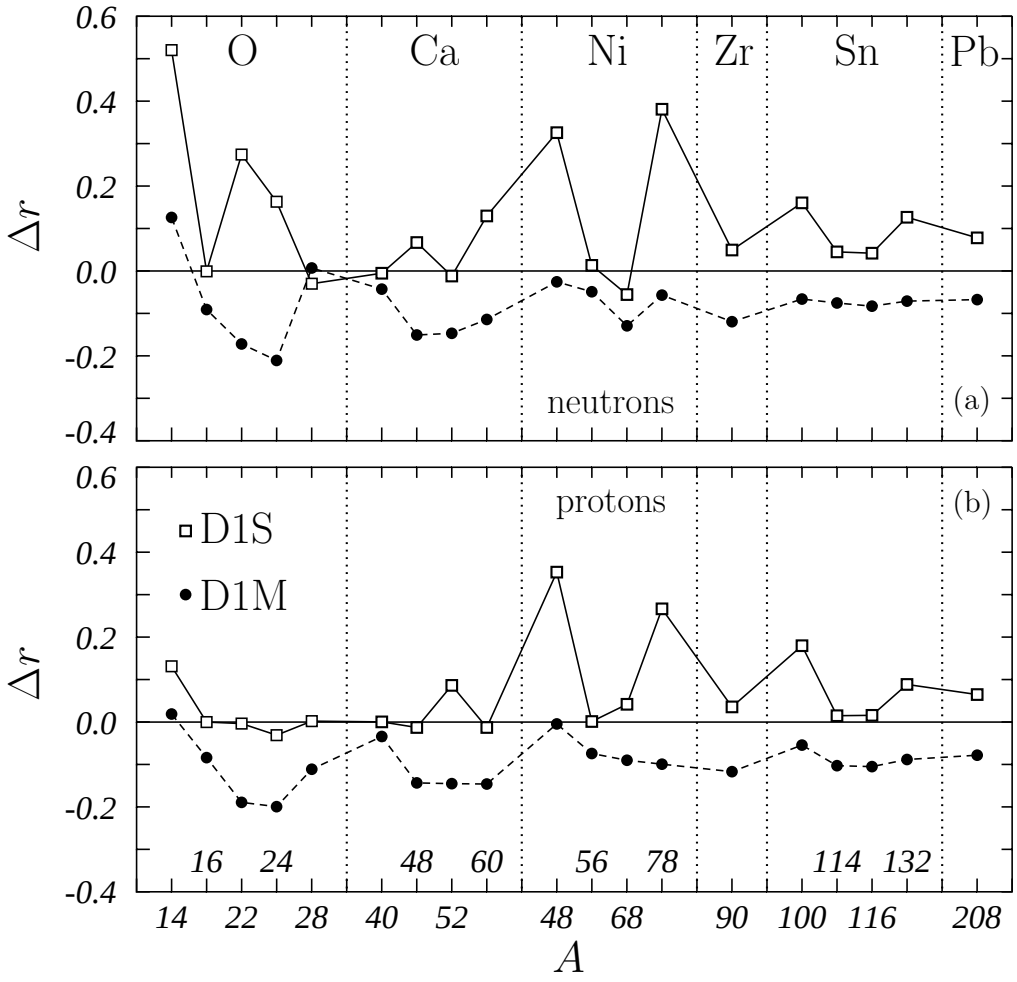

Figure 4: Relative percentage difference, Eq. (5), between root mean square radii of neutrons (upper panel) and protons (lower panel) distributions calculated with and without tensor for D1ST and D1S (open squares) and D1MT and D1M (solid circles) interactions.

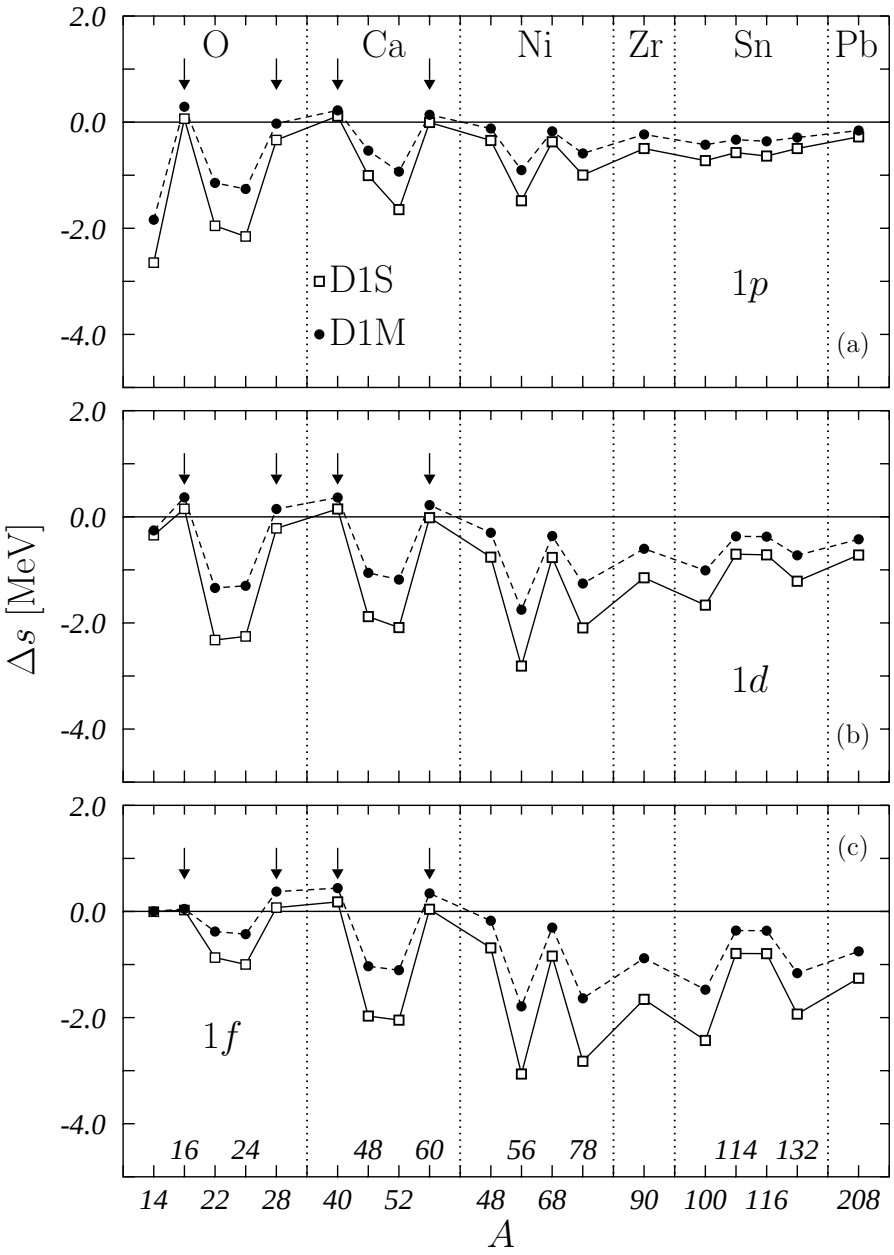

Figure 5: Differences between the s.p. energy differences of spin-orbit partners levels, Eq. (7), calculated with and without tensor forces, for the $1p$, panel (a), $1d$, panel (b), and $1f$, panel (c), proton states. The results for D1S and D1ST interactions are shown by open squares and solid circles, respectively. The arrows indicate those isotopes where the effect of the tensor is expected to be zero.

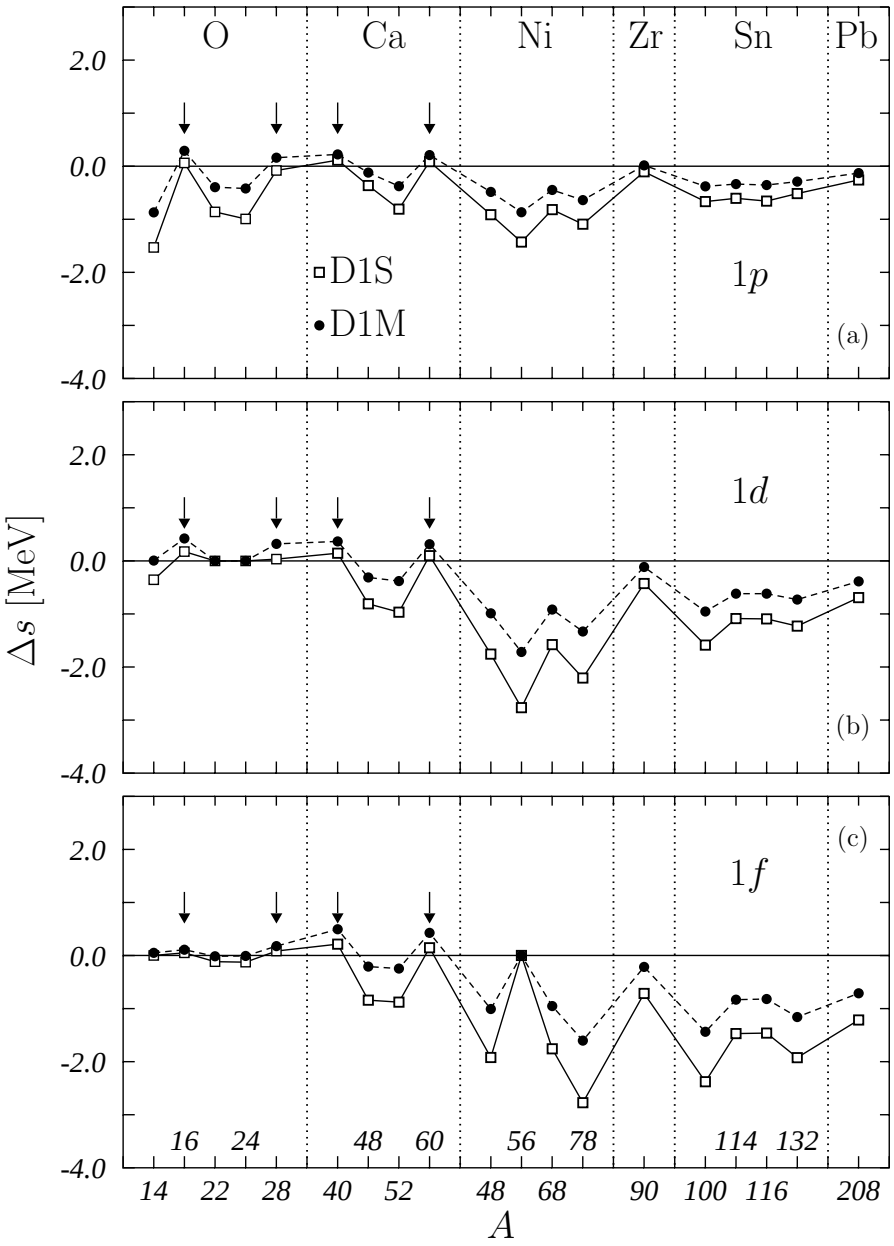

Figure 6: The same as Fig. 5 for neutron states.

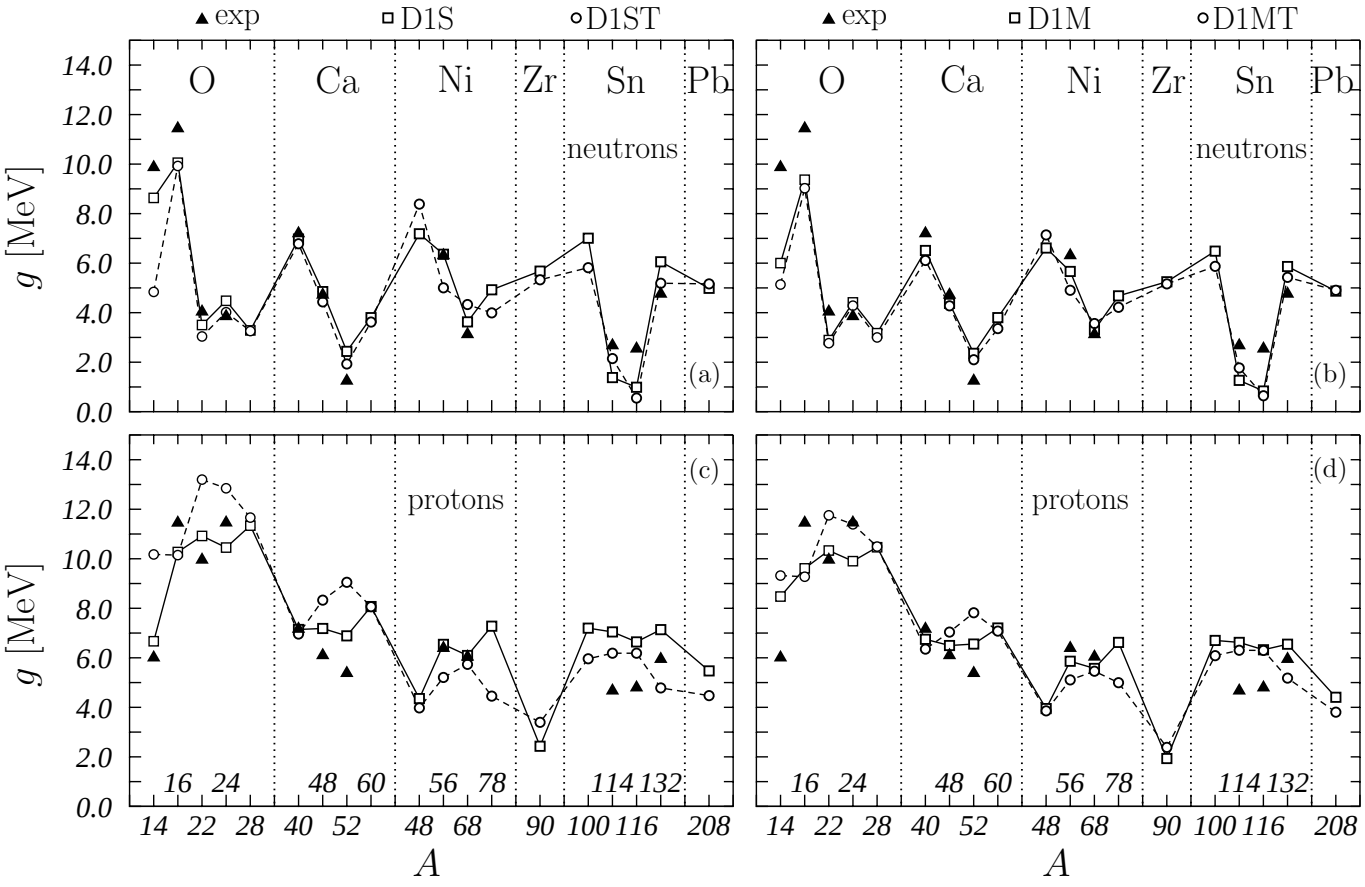

Figure 7: Neutron, panels (a) and (b), and proton, panels (c) and (d), energy gaps, in MeV, for the various nuclei and interactions we have investigated. In the left panels we show the results obtained by using the D1S interactions and in the right panels those obtained with the D1M forces. The experimental values, solid triangles, have been extracted from the binding energies of the neighbouring nuclei [39, 40].

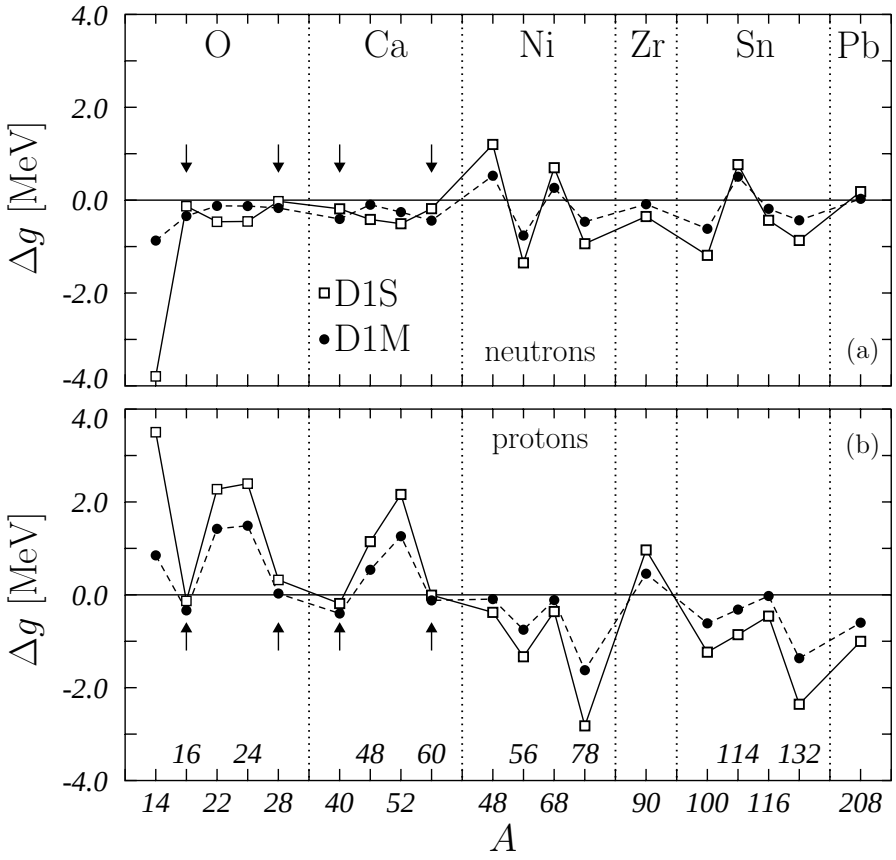

Figure 8: Differences between the energy gaps calculated with and without tensor force, for neutrons, panel (a), and protons, panel (b). The results obtained with the D1S type interactions are indicated by the open squares, and those obtained with the D1M type interactions by the solid circles. The arrows indicate those isotopes where the tensor effect is expected to be zero.

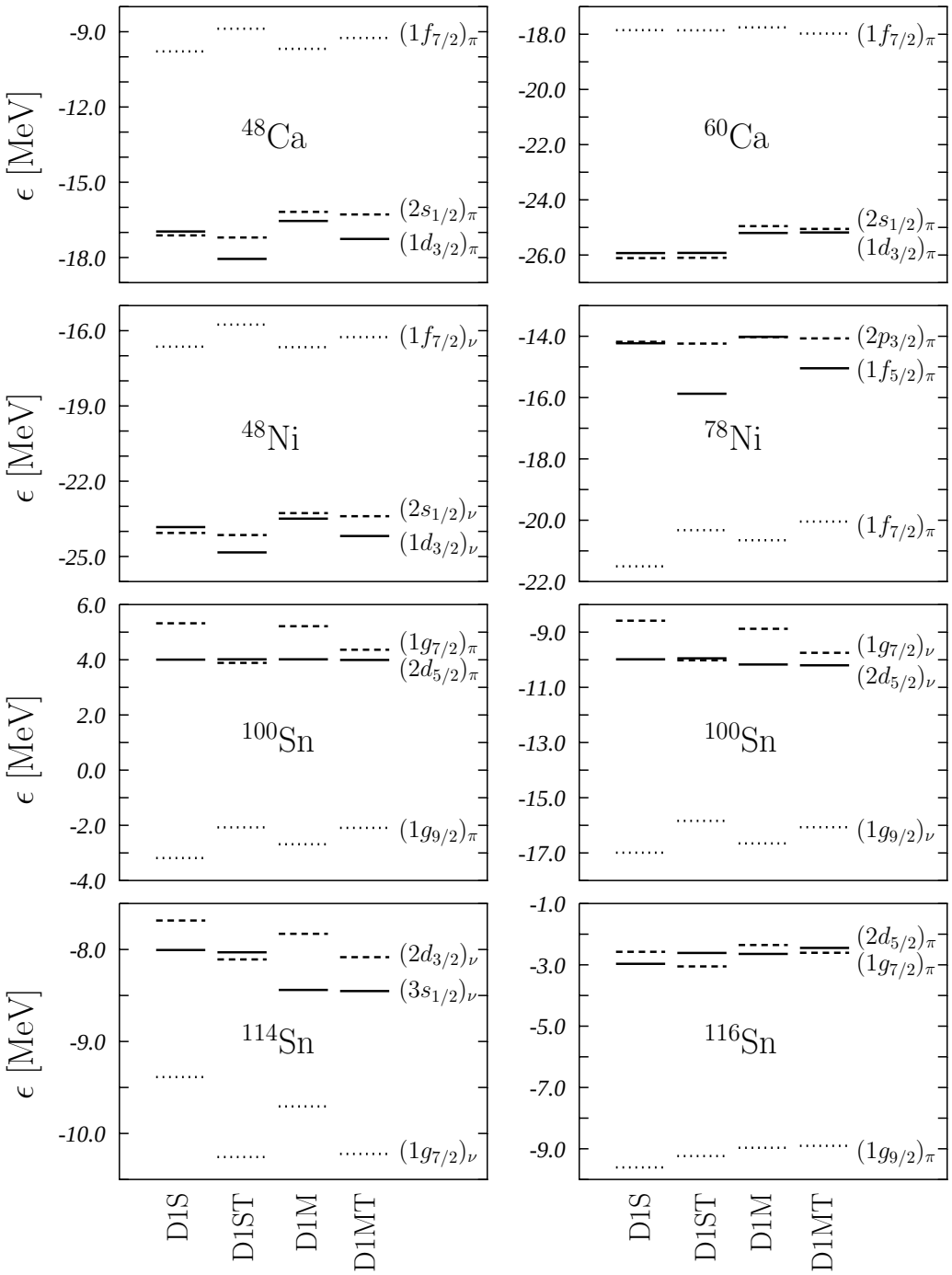

Figure 9: Single particle levels around the Fermi surface which change their order when the tensor force is used.

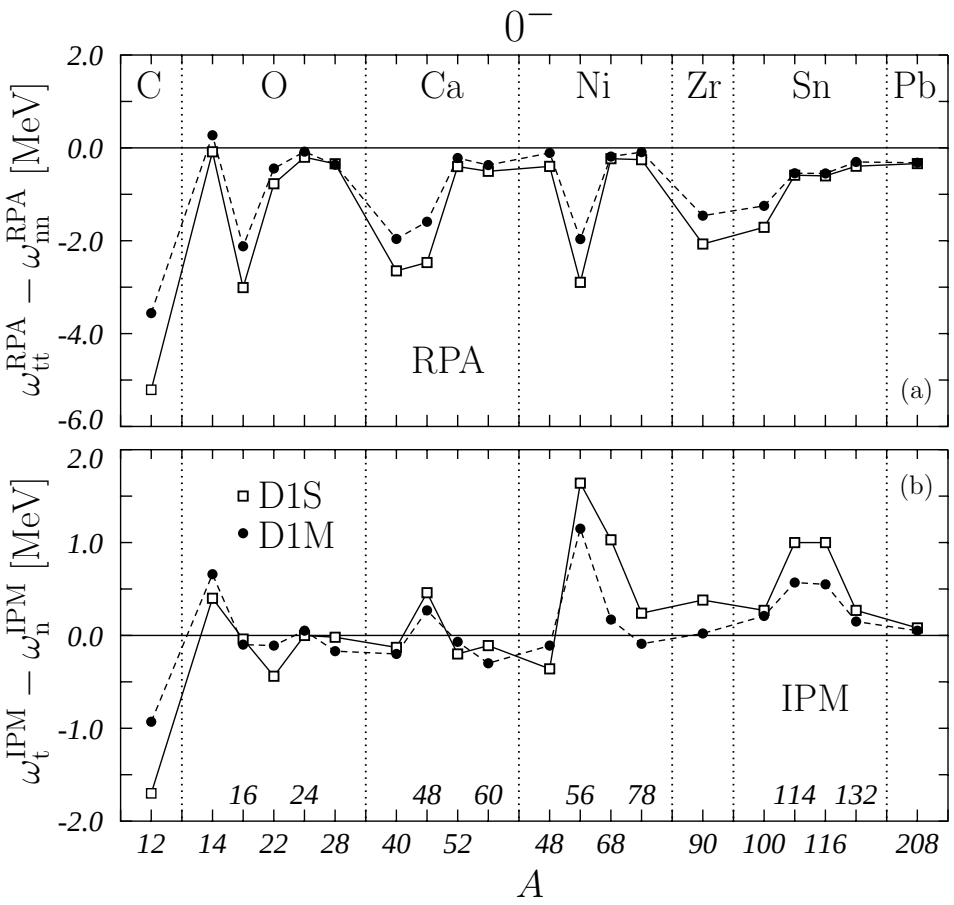

Figure 10: Differences between the energies of the first 0^- excited state obtained with and without tensor forces, for the nuclei under investigation. D1S (D1M) results are plotted with open squares (solid circles). In the panels (a) and (b) we show the results obtained with RPA and IPM calculations, respectively.

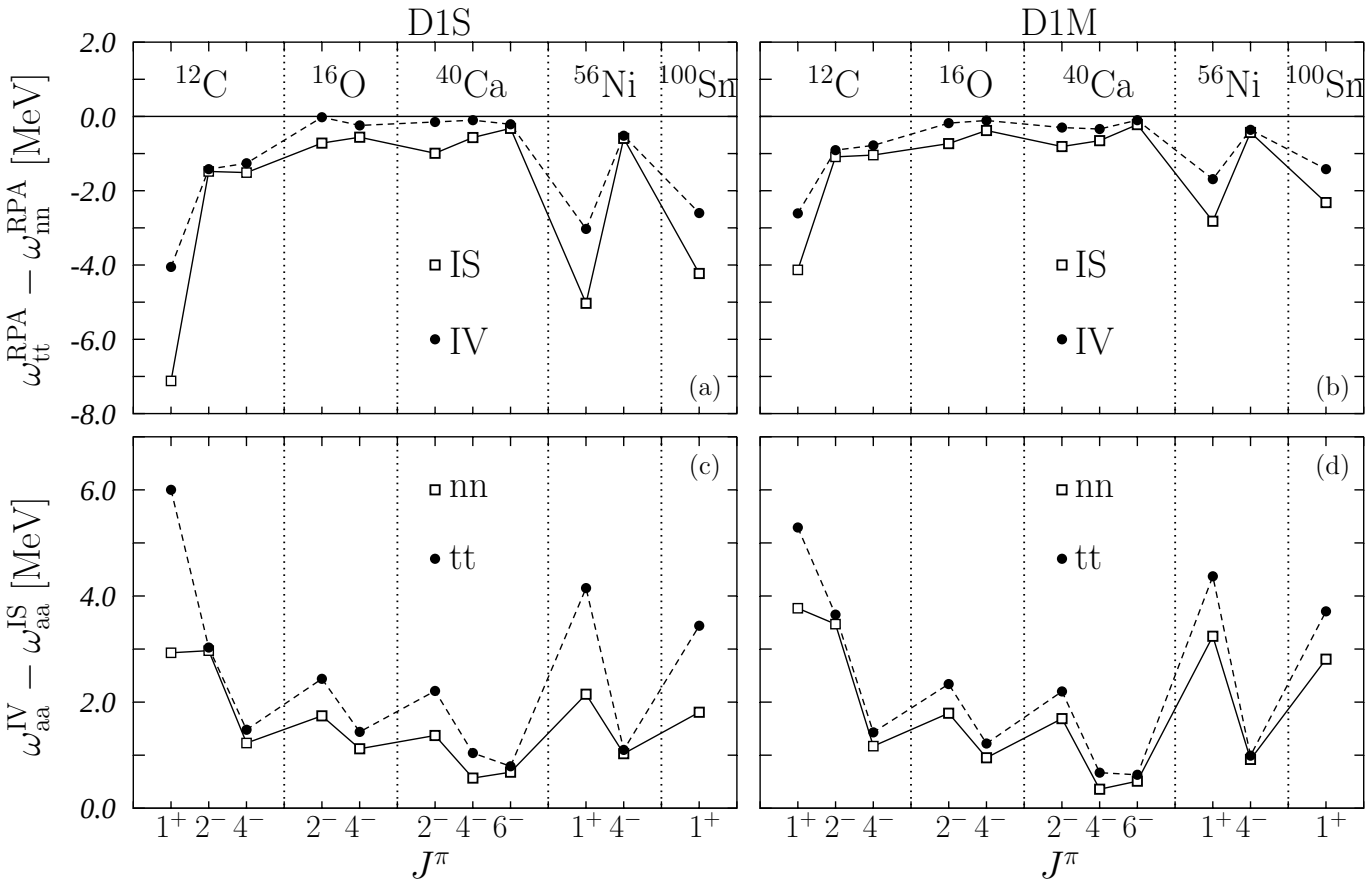

Figure 11: In the panels (a) and (b) we show the differences between the energies calculated with and without tensor terms for the IS and IV states listed in Table II. In the panels (c) and (d) we show the differences between the energies of the IV and IS states obtained in fully self-consistent RPA calculations with and without tensor forces. In the panels (a) and (c) we show the results obtained with the D1S type forces, and in the other two panels those obtained with the D1M type forces.

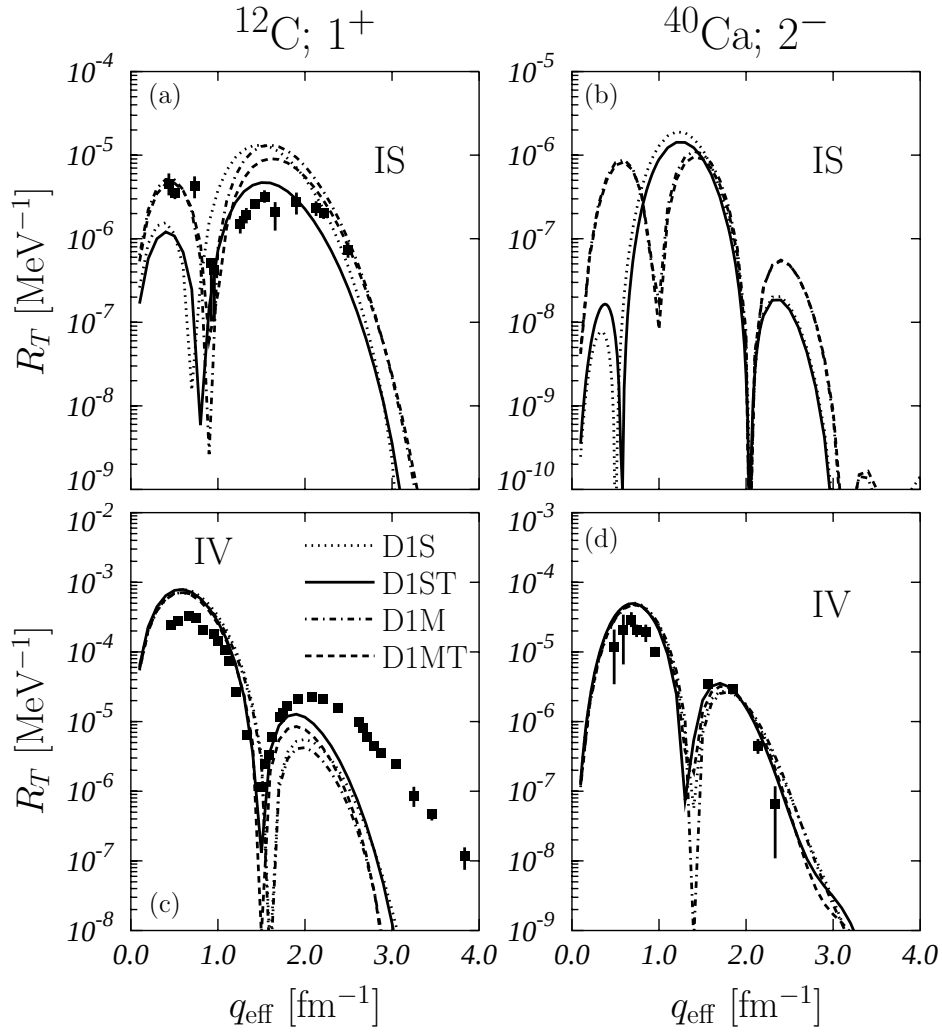

Figure 12: Inelastic electron scattering transverse response as a function of the effective momentum transfer [44], calculated by using RPA wavefunctions obtained in fully self-consistent calculations done with different interactions. The data are from Refs. [45, 46].

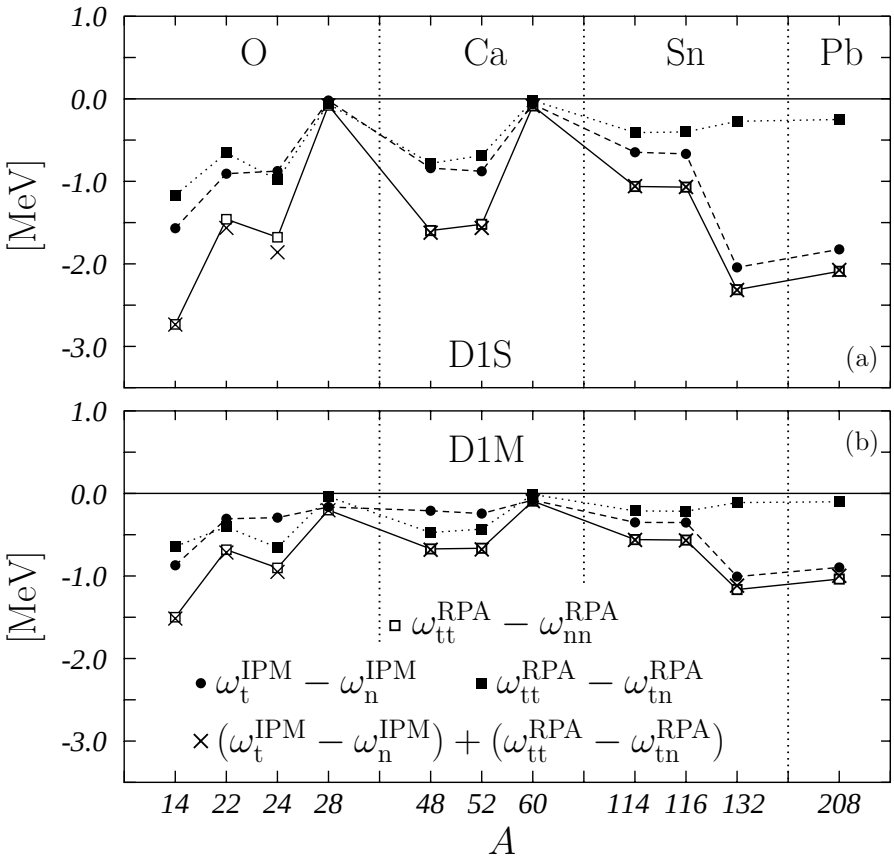

Figure 13: Differences between the energies of the 1^+ excitations having the largest $B(M1)$-value, in various nuclei. Solid circles indicate the results obtained in the IPM by using s.p. wave functions and energies obtained in HF calculations done with and without tensor. The solid squares show the results obtained in RPA calculations with and without tensor force, using the s.p. wave functions and energies obtained in HF with tensor force. The crosses show the sum of the two previous results. Open squares show the energy differences obtained by doing complete self-consistent calculations where the tensor force is used or not in both HF and RPA calculations.

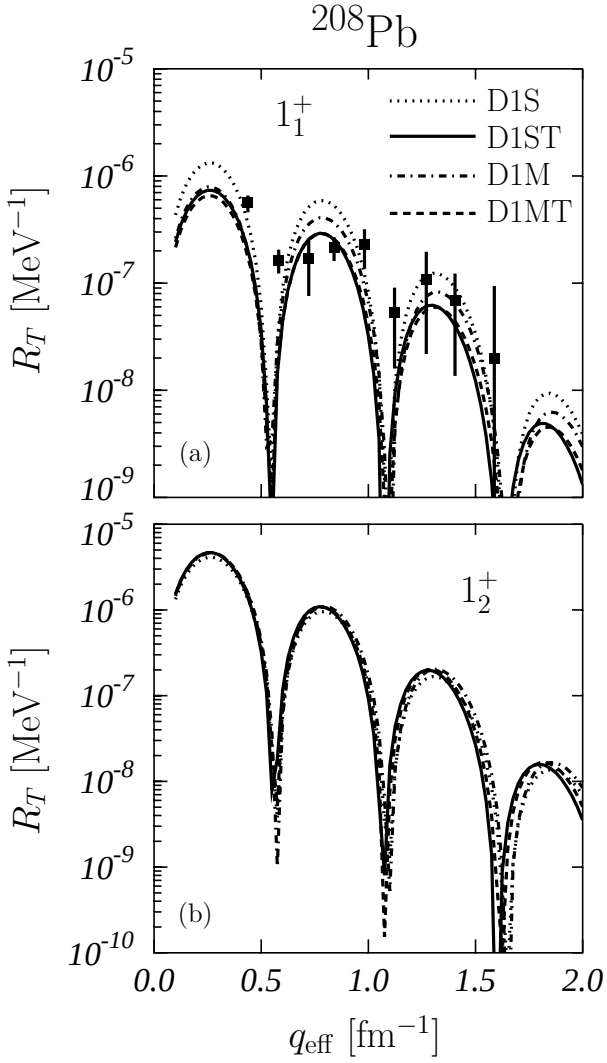

Figure 14: Inelastic electron scattering transverse responses as a function of the effective momentum transfer [44], calculated by using RPA wavefunctions obtained in fully self-consistent calculations done with different interactions. In panel (a) we show the results obtained with the RPA wavefunctions of the lowest excited states. The RPA wave functions used to obtain the results shown in panel (b) are those of the second excited state. The experimental data are from Ref. [48].